University of Baghdad
College of Engineering
JOURNAL OF ENGINEERING

# Journal of Engineering

journal homepage: www.joe.uobaghdad.edu.iq

Volume 29 Number 12 December 2023

# Performance Assessment of Pile Models Chemically Grouted by Low-Pressure Injection Laboratory Device for Improving Loose Sand

**Mohammed Saleh Mohammed [1,*], Mahmood D. Ahmed[2]**

Department of Civil Engineering, College of Engineering, University of Baghdad, Baghdad, Iraq
m.mohammed1901p@coeng.uobaghdad.edu.iq[1], dr.mahmood.d.a@coeng.uobaghdad.edu.iq [2]

## ABSTRACT

The complexity and partially defined nature of jet grouting make it hard to predict the performance of grouted piles. So the trials of cement injection at a location with similar soil properties as the erecting site are necessary to assess the performance of the grouted piles. Nevertheless, instead of executing trial-injected piles at the pilot site, which wastes money, time, and effort, the laboratory cement injection devices are essential alternatives for evaluating soil injection ability. This study assesses the performance of a low-pressure laboratory grouting device by improving loose sandy soil injected using binders formed of Silica Fume (SF) as a chemical admixture (10% of Ordinary Portland Cement OPC mass) to different (W/C) water/cement ratios (by mass materials) mixes. Trial grouting processes were executed to optimize the practical ranges of the operating factors of the laboratory device to obtain consistent grouted model pile samples. The paper examined the relations of the binders' W/C ratios with the densities, elasticity modulus ($E$), and Uniaxial Compression Stress (UCS) of the grouted piles. The investigation results show that as the binder W/C ratio rises, the grouted pile samples' dry density, $E$, and UCS values decrease. For the binder injected with a W/C ratio of one and 10% SF additive by weight of cement mass, the highest values of the grouted pile for density, $E$, and UCS were about 2.32 g/cm$^3$, 23 MPa, and 2000 MPa, respectively. The UCS of the grouted pile proved that the binders' W/C ratios and the SF addition have an evident effect on the investigated factors of the grouted piles.

**Keywords:** Jet grouting, Grouted piles, Silica Fume, Chemical additive, W/C ratio.

*Corresponding author
Peer review under the responsibility of University of Baghdad.
https://doi.org/10.31026/j.eng.2023.12.08

Article received: 10/04/2023
Article accepted: 17/08/2023
Article published: 01/12/2023

# تقييم أداء نماذج ركائز محقونة كيمياوياً بجهاز مختبري واطئ الضغط لتحسين تربة رملية رخوة

**محمد صالح محمد[1]*، محمود ذياب أحمد[2]**

قسم الهندسة المدنية، كلية الهندسة، جامعة بغداد، بغداد، العراق

**الخلاصة**

التعقيد والطبيعة المعزّفة جزئياً لحقن التربة بالسمنت تجعل من الصعب توقع أداء ركائز الحقن. لذلك فإن أعمال الحقن بالسمنت التجريبية لموقع بنفس خواص تربة موقع الإنشاء هو ضروري لتقييم أداء ركائز الحقن. لكن بدلاً من تنفيذ ركائز حقن تجريبية في موقع تجريبي والتي هي ضياع للمال والوقت والجهد فإن أجهزة الحقن المختبرية تعتبر بديل أساسي في تقييم قابلية حقن التربة. هذه الدراسة تُقيّم أداء جهاز حقن مختبري واطئ الضغط لتحسين تربة رملية رخوة تم حقنها بمواد رابطة مكونة من رغوة السيليكا كمضاف كيمياوي (نسبة 10 % من وزن السمنت البورتلاندي) لخلطات ذات نسب ماء الى سمنت مختلفة.

تم إجراء تجارب حقن تجريبية لإيجاد أمثل مدى لقيم عملية للعوامل التشغيلية لجهاز الحقن المختبري للحصول على نماذج ركائز حقن متجانسة. درست علاقة نسب الماء/السمنت (نسبة وزنية) لمواد الحقن مع الكثافة ، معامل المرونة ومقدار الإنضغاط غير المحصور للركائز المحقونة. برهنت النتائج أنه عندما تزداد نسبة الماء/السمنت للمادة الرابطة فإن قيم الكثافة، معامل المرونة وفحص الإنضغاط غير المحصور لركائز الحقن تقل. لمادة حقن بنسبة ماء/سمنت بمقدار1 مع نسبة رغوة السليكا كمضاف بمقدار 10% من وزن السمنت فإنه يتم الحصول على أعلى قيم للكثافة ، معمل المرونة وفحص الإنضغاط غير المحصور لركائز الحقن بحدود 2,32غم/سم3 ،23 ميكاباسكال و2000 ميكاباسكال على التوالي. إن قيم فحص الإنضغاط غير المحصور برهنت بأن نسبة الماء/السمنت وإضافة رفوة السيليكا لها تأثير واضح على الخواص التي تم دراستها للركائز المحقونة.

**الكلمات المفتاحية :** الحقن بالبثق ، ركائز الحقن، رغوة السيلكا، المضاف الكيمياوي، نسبة الماء/السمنت.

## 1. INTRODUCTION

Soil improvement can improve bearing capacity, shear strength, and density, convey loadings to more stable strata, minimize deformations, decrease applied loadings, speed up consolidating, provide lateral stability, fill voids or form seepage cutoffs, and enhance liquefaction resistance **(Schaefer et al., 2012; Han, 2015; Kumar et al., 2020)**.

Because the rate of urbanization on problematic soils is increasing, soil improvement methods have become more prevalent in construction projects. Jet or high-pressure grout may be used in every soil type. Jet grouting involves using a high-pressure jet (at least 300 bar) to cut the soil and partly replace it with grout. The stabilizer is made up of varied proportions of water and cement. The water-cement combination accumulates significant velocity or kinetic energy while flowing through the nozzles on the jet-grout equipment. This results in a soilcrete mass with strength properties independent of the original soil fabric **(Wang et al., 2013; Akln et al., 2015; Njock et al., 2018; Guler et al., 2021)**.

Jet grouting is a complex process. Therefore, little is known about it. Grouted pile grade is difficult to estimate and control. Jet grouting experiments are usually needed to evaluate cement injection on a given soil type. Jet grouting experiments are done in the same geotechnical conditions as the principal erection site. It's essential to grout various piles with different operating variables. Test piles are dug after cement injection for visual inspections and other testing. Trial-jet grouting isn't always effective. It's time-consuming, expensive, and may not work. To replace field grouting experiments, the laboratory jet grouting configuration was required **(Nikbakhtan, 2015; Mohammed et al., 2023).**

SF is a highly reactive pozzolanic material for the chemical reactions between reactive silica in the SF grains and calcium hydroxide produced from cement hydration in the water at ambient temperature. Adding the SF to the W/C mix results in the presence of billions of microscopic particles. Like sand fills the pores among gravel particles, SF plugs for the spaces between cement grains. The micro-filler effect would improve the grouted pile properties even if SF did not react chemically **(Holland, 2005; Reddy, 2017).**

The reactive silica in the SF particles reacts with the calcium hydroxide formed during cement hydration in the water presence at room temperature, making SF a highly reactive pozzolanic material. The pozzolanic (S) in the SF combines with this Calcium-Hydroxide ($CH$) to form an extra-binding substance called Calcium-Silicate-Hydrate ($SCH$), which is comparable to the Calcium-Silicate-Hydrate ($SCH$) hydrated from PC. The added binder is mainly responsible for the enhanced hardening qualities of SF concrete Eqs. (1) to (4) **(Muller et al., 2015; Hasanzadeh and Shooshpasha, 2019; Olgun et al., 2021)**.

$$Cement + Water \rightarrow Calcium\ Silicate\ Hydrate\ + Calcium\ Hydroxide \quad (1)$$

$$(C_2S\ \&\ C_3S) + (H) \rightarrow (SCH) + (CH) \quad (2)$$

$$Pozzolan + Calcium\ Hydroxide\ + Water \rightarrow Calcium\ Silicate\ Hydrate \quad (3)$$

$$(S) + (CH) + (H) \rightarrow (SCH) \quad (4)$$

**(Karkush et al., 2018)** studied how permeating grout affected the UCS of soft clay soil with low plasticity from the Al-Jadryiah area in Baghdad. The soil samples were improved by grouted gel of cement/water with three weight percentages. In addition to cement injection, soil samples were enhanced with SF at 2 and 4 %. After grout, the improved soil samples were left to dry for 1, 3, and 7 days. Tests showed that increasing grouting gel % increased UCS and decreased axial strain. SF increased UCS and reduced axial strain in soft, clayey soil enhanced by the cementing agent.

**(Al-Malkee and Ahmed, 2021)** studied how the W/C ratio affects grouted piles' mechanical and physical properties. To assess their properties, coarse soil samples with various water/cement ratios were examined at multiple curing durations. The results show that the (UCS) of grouted pile reduces with rising grout (W/C) ratio, where the grouted pile strength of a W/C ratio of 0.7 is higher than about 237 % of a water/cement ratio of 1.4 at 28 days; the growth of UCS is proportional to the logarithm time of curing; the ratio between the tangent modulus ($E_{tg50}$) to 50% of the ultimate UCS of grouted pile) varies from 113 to 175 %, and the dry density of the grouted pile rises as the W/C ratio increases.

**(Ali and Yousuf, 2016)** investigated the influence of permeation injection using fly ash to improve sandy soil from Karbala City in two phases. The first phase concerned the shear strength, while the second was the grouting materials' effect on the grouted zone's volume by injection. The study improved sand with fly ash as a replacement substance for cement (3 W/C ratios) in weight percentages of 10 %, 25 %, and 40%. The study results showed that after one day of curing, the shear strength and approximate volume of the effective injected zone of the improved samples were raised with a reduction in the W/C ratio.

**(Fattah et al., 2020)** performed research to stabilize sand by grouting a lime-silica fume (L-SF) slurry. The dune sand specimens were collected from north Iraq and subjected to erosion experiments utilizing centrifugal fans with a wind speed of 90 km/h for 11 minutes. Stabilization using silica fume (SF) and an L–SF mix was tested on dune sands. Mixing dune sand with L-SF slurry reduced erosion by 70% using a stabilizer grout of 33% (Lime to SF ratio, 3L: 4SF) and 67% water to the total mix mass. The number and depth of grout holes surrounding the stabilizing region boosted stability. Wind at 90 km/h for 11 minutes caused 66 mm of erosion on natural sand dunes, whereas L-SF-stabilized soil showed 17–36 mm of erosion. Increasing injection locations and decreasing their spacing minimized soil erosion.

**(Fattah et al., 2013)** performed research to grout four gypseous soils with varying properties and gypsum concentrations. Remolded samples were used to study gypseous soil compressibility under various conditions. The specimens were injected using acrylate liquid. The studied parameters were the grouting pressure, the flow radius, the injection time, and the acrylate liquid quantity. The treated samples revealed that acrylate liquid reduced gypseous soil compressibility by 60–70%. This is because the acrylate liquid sheet protects the gypsum grains from water. The acrylate liquid decreased the collapsibility of treated gypseous soil by 50–60%. Acrylate liquid increases cohesion and reduces internal friction in gypseous soil, affecting shear strength parameters.

**(Al-Saidi et al., 2022)** investigated the impact of injection lime (L), silica fume (SF), and lycopod-h (LH) on soft clay consolidation settlement. A natural soft clayey soil laboratory sample was injected with the grout materials (L, SF, L + SF, and L + SF + LH). The effect of injection hole spacing and grout depth was examined. A (L + SF + LH) slurry injected into the soft clay under or around the footing enhanced bearing capacity by 5–88%. Due to the shape of the shear failure of the soft clay around the footing, injection near the footing at 0.5 diameter is more effective than grouting at 1.0 diameter.

This experimental study aimed to develop and locally manufacture a low-pressure grouting laboratory device with a similar act to the field machinery but on a smaller scale. Model piles were injected with binders composed of silica fume with 10% of the ordinary Portland cement mass as a chemical admixture to different W/C mixtures to improve the loose (Dr =20 %) sandy soil from Karbala governorate. Trial grouting processes were performed to optimize the practical limits of the operating factors (binder grout pressure/discharge, amount of injection nozzles and their size, penetrating/lifting rate, and revolution speed of the boring-grouting rod) of the laboratory device to obtain consistent grouted pile samples. Within the scope of this study, the correlation between the W/C ratios of the binders and the densities, elasticity moduli, and uniaxial compression stresses of the grouted pile models was investigated after performing the unconfined compressive tests UCTs program.

## 2. MATERIALS AND METHOD

## 2.1 Materials

The improved soil was loose with Dr =20 % poorly graded sand with few fines passing through sieve size 10, and its properties are given in **Table 1**. **Fig. 1** illustrates the soil particle size distribution curve. The soil testing boxes are prepared in the following stages:

**Table 1.** Properties of the investigated soil

| Characteristics of sand | Value | Standard or specifications |
|---|---|---|
| Specific gravity ($G_s$) | 2.65 | ASTM-D854-14 |
| Max. dry unit weight ($\gamma_{d\,max}$), kN/m$^3$ | 18.51 | ASTM-D4253-14 |
| Min. dry unit weight ($\gamma_{d\,min}$), kN/m$^3$ | 16.85 | ASTM-D4254-16 |
| Maximum void ratio ($e_{max}$) | 0.57 | Soil phase relationships calculation |
| Minimum void ratio ($e_{min}$) | 0.43 | Soil phase relationships calculation |
| Uniformity Coefficient ($C_U$) | 2.36 | Poorly graded soil ($C_U$ < 6) |
| Curvature Coefficient ($C_C$) | 0.98 | Poorly graded soil ($C_C$ not in the range 1-3) |
| Fines % | 0.6 | ASTM-D6913/D6913M-17 |
| Plasticity index | NP. | ASTM-D4318-17 |
| Soil classification (USCS) | SP | ASTM-D422-63(2007)+ ASTM-D2487-11 |
| Soil relative density (Dr %) | 20 % | Regarding the study necessities |
| Dry unit weight ($\gamma_d$), kN/m$^3$ | 17.16 | Computed from Equation(5) |
| Saturated unit weight ($\gamma_{sat}$), kN/m$^3$ | 20.7 | Soil phase relationships calculation |
| Void ratio | 0.54 | Soil phase relationships calculation |
| Dry friction angle, $\emptyset^\circ$ | 31 | D3080/D3080M- 11 |
| Saturated friction angle, $\emptyset^\circ_{sat}$ | 27 | DST/undrained condition |
| Oedometer Elastic modulus ($E_{od}$), MPa | 13 | ASTM-D2435/D2435M-11 |

- The pluviation deposition method (**Figs. 2 and 3**) is used to reconstitute homogeneous and repeatable densities of sand layers with the required relative density, where the corresponding dry unit weight is calculated based on Eq. (5) using the maximum and minimum dry laboratory unit weights **(Lambe, 1991).**

$$D_r = \frac{\gamma_d - \gamma_{d\,min}}{\gamma_{d\,max} - \gamma_{d\,min}} \times \frac{\gamma_{d\,max}}{\gamma_d} \times 100 \quad (5)$$

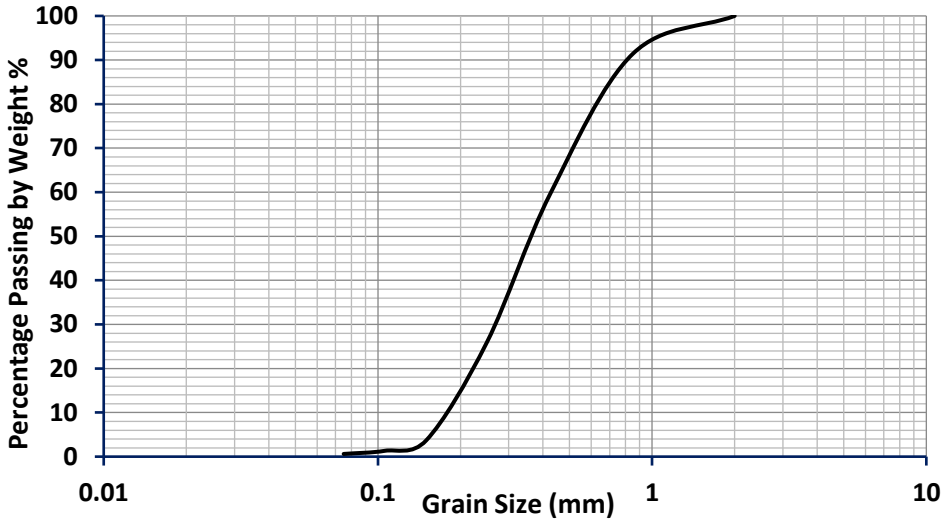


**Figure 1.** Particle size distribution for the investigated soil

**Figure 2.** Raining model box from elevated elevated hopper funnel for soil preparing

**Figure 3.** Raining model box using diffuser screen for soil preparing

where $D_r$, $\gamma_d$, $\gamma_{d\ max}$, and $\gamma_{d\ min}$ are the selected soil relative density, the selected dry unit weight, the soil dry unit weight in densest conditions, and the soil dry unit weight in loosest conditions, respectively.

- From the required (calculated from Eq. (5)) dry unit weight and sand bed volume, the required dry sand weight is pluviated inside the soil box in the continued path of adjacent parallel lines in a specific direction of the model test (either in a long or short direction), where the sand of the subsequent layer is likewise pluvial but in a perpendicular direction **(Fretti, 1995; Hariprasad et al., 2016; Hossain and Ansary, 2018)**.
- A hopper funnel with a 0.4 m diameter and 0.35 m height suspended at (0.9-3) m elevation by a 1-ton hydraulic engine crane provides a continuous flow of sand. This raised funnel is

connected to a reinforced flexible plastic hose with a 5 mm diameter that ends with a diffuser screen so that uniform sand beds can be spread along the parallel contours marked on the inside of the model box, which is manufactured of steel and has a transparent polycarbonate visible sheet.

- After sand pluviation of each bed, the surface is finished to the needed elevation, shown by lines drawn on the sides of the sample box with gentle tamping for layers reconstitution.
- After completing the preparation of the sample box, a one-inch-thick sandwich plastic panel was bored with the required radius and circle amounts for the pile models to be injected, and a thin sheet of polythene was placed beneath this sandwich layer to prevent the infiltration of spoiled binder into the sample box during the grouting process. In the injection procedure, a small portion of this polythene sheet is eliminated sequentially with each low-pressure injection of the pile model.

## 2.2 Low-Pressure Laboratory Injection Process

As shown in **Figs. 4, 5, and 6,** the parts that comprise the low-pressure grouting laboratory device were purchased from regional industry suppliers and assembled by the study's researcher according to the required design.

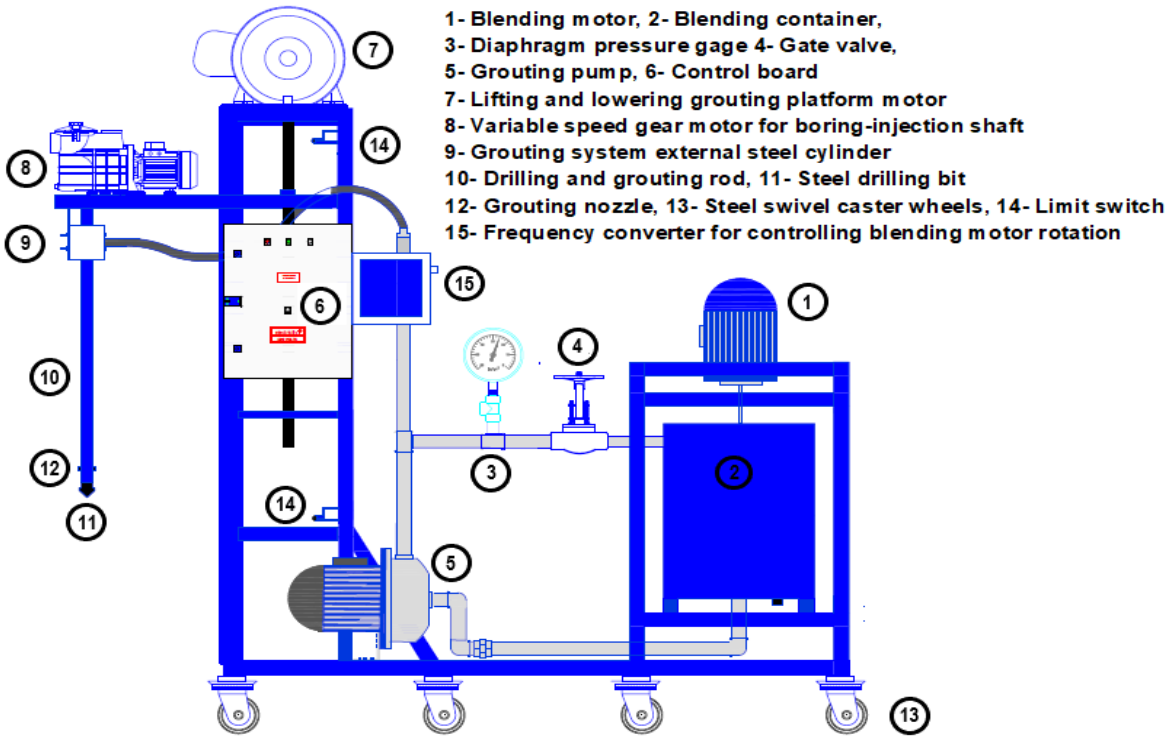


**Figure 4.** Schematic diagram of the low-pressure grouting laboratory device that was used in the study **(Hussein and Ahmed, 2023)**

After the soil preparation was complete, many experimental grouting trials were performed to get consistent pile models by determining the best ranges of operational grouting factors (the boring and grouting shaft rotation rate in rev/min and penetrating/withdrawal rate in cm/min., the binder fluid pressure in kPa and rate of flow in l/min., and the quantity and diameter of the grouting nozzles). The following steps are needed to perform soil

improvement by producing homogeneous and uniform experimental low-pressure grouted pile models:

- After mixing the grouting materials in the right amounts in a separate bucket with a portable electric hand mixer, the grouting fluid is emptied into the blending container of the low-pressure injection device. Then, the blending motor starts to operate to the appropriate rotation rate by the three-phase adjustable-frequency driving inverter on the controlling board.
- To ensure that the grouting pumping works appropriately, the grouting fluid is circulated starting from the base of the blending container via the setup pipe scheme and back to the upper entry of the blending container.

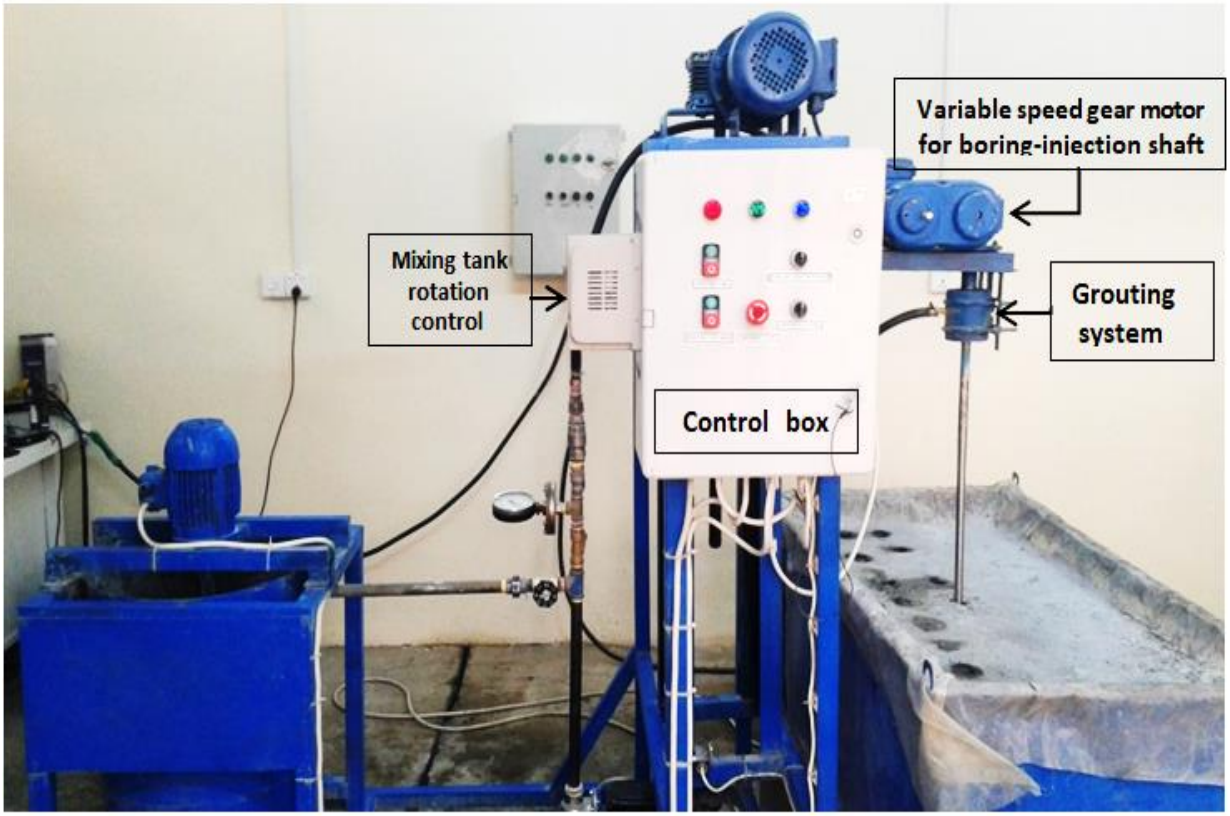


**Figure 5.** Laboratory low-pressure injection device with the soil box during low-pressure injection process **(Hussein and Ahmed, 2023)**

- The drilling-grouting shaft is then rotated clockwise at 50 revs per minute and lowered to the sandbox at 0.20 m per minute.
- Before starting the low-pressure grouting process, a trial grouting (grouting a small quantity of binder over the surface of the soil) is made to guarantee the nozzles' correct action. This trial grouting is important to ensure that nozzles are not clogged by soil particles meddling and that the grouting keeps going while the soil is bored and grouted.

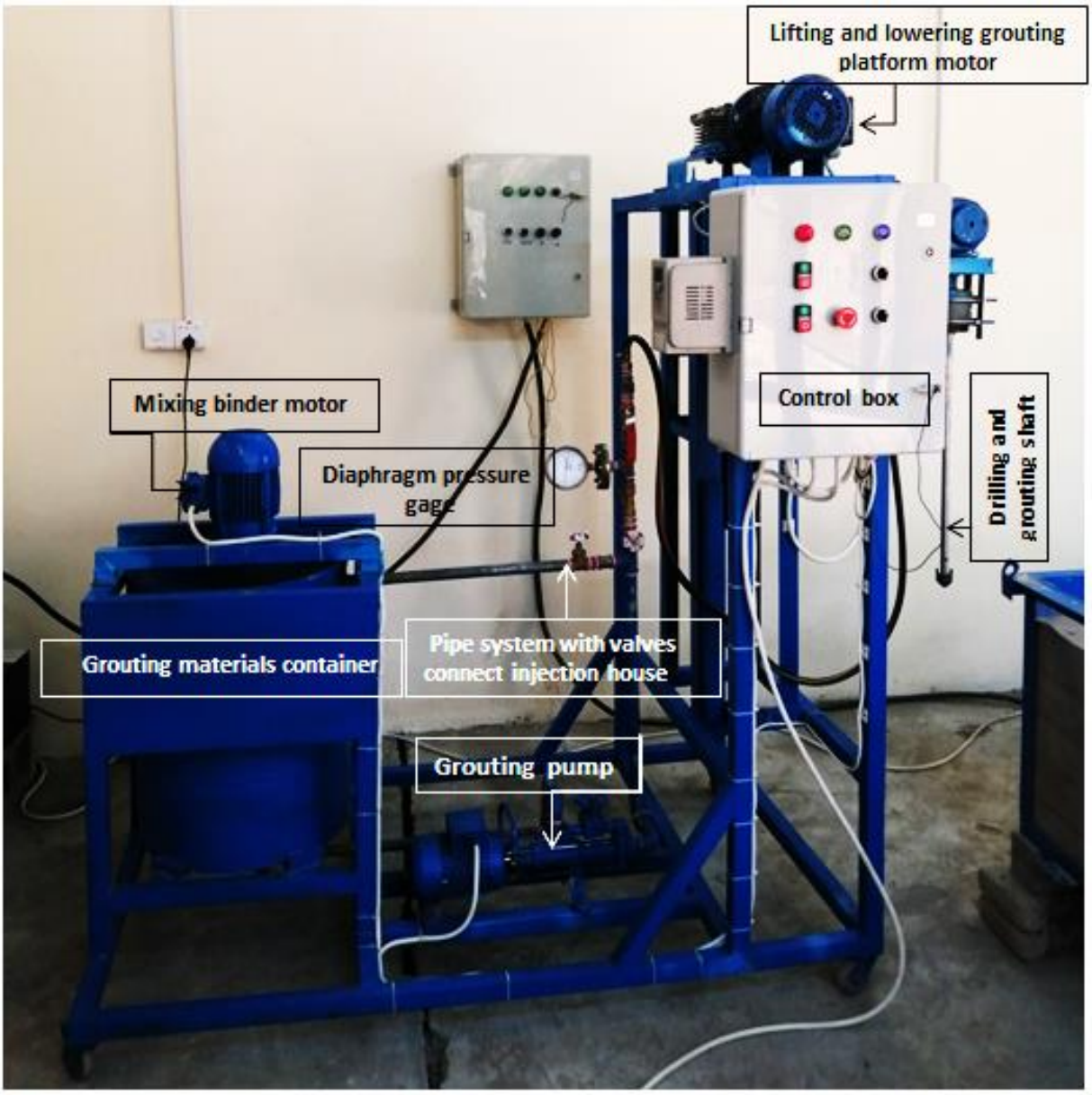


**Figure 6.** Laboratory low-pressure injection device with the main parts marking **(Hussein and Ahmed, 2023)**

- The low-pressure injecting process is performed in two stages in the soil box (by heading the platform injection scheme down and rotating the boring and grouting shaft in a clockwise rotation):
  -The first step relates to the down-boring procedure of the grouting hole with an appropriate binder grout pressure for stabilizing the hole walls.
  -The additional step (main procedure) begins following the boring and grouting shaft reaching the hole base in the sample container. On the controlling board, the shaft rotating is inverted in the anticlockwise rotation, and the platform injection scheme is heading upward at the earlier suggested rotation rate with the necessary grouted pressure of binder based on the diaphragm pressure gauge.
- Through the low-pressure grouting procedure, some binder flow spoiled from the grouting hole surfaces to be removed from the box sample surface.

- The drilling-grouting scheme platform moves upward until the nozzles reach the sample box's surface in the low-pressure grouting procedure. This completes the low-pressure soil injection process, which produces homogenous and consistent injected pile models.
- In the low-pressure grouting process, there is a small depression on the pile models' surface (densifying for the laboratory grouting process makes the pile models shorter), filled with identical sand properties, and admixed with the upward spoiled binder.
- The laboratory grouting procedure lasted by moving the setup to a new position in the box sample till the necessary amount of **(Fig. 7)** pile models had been grouted.
- Next, the pile model laboratory grouting process is accomplished, the curing period begins, and the next stage is started by moving the soil box to the shaking table tests.
- Some pile model samples **(Fig. 8)** were randomly selected to perform the UCTs after immersion in an appropriate water container for the required curing period.
- Next, the UCTs are executed on sample groups (3 samples with a diameter of about 40 mm and a height between 2 and 2.5 times the Dia.) from randomly chosen model piles.
- Each sample group was tested for each W/C ratio. The binder used for low-pressure laboratory injection in these pile models is silica fume with 10% of the ordinary Portland cement mass mixed as a chemical additive with various W/C ratio mixtures.

**Figure 7**. Pile models for UCTs in the soil box after completion of the injection process

**Figure 8**. (40-80 mm Dia. with 300 mm) long pile models after a 28-day curing

## 3. RESULTS AND DISCUSSION

This study utilized an automated loading device with a maximum capacity of 50 kN supplied with a calibrated electronic load cell and data logger for data acquisition to perform the unconfined compression tests. To define the ultimate applied load, the specimens were centrally loaded at a 1.2 mm/min displacement rate until failure, according to **ASTM-D2166**. The tests were conducted on identical specimens for all binder collections to lessen the variance in test circumstances and substances. The results were verified since the data error was less than 5 %. A high determination coefficient ($R^2$) for grouted pile UCS with the W/C ratios, elasticity modulus, and dry density relations was obtained using the CurveExpert Professional program version (2.7.3) to generate accurate calculations utilizing a cross-platform solution for data analysis and curve fitting.

The examined relations in the laboratory study were the dry bulk density, the average (UCS), and the ($E$) of the grouted pile samples with the W/C ratio of the injected binder, as shown in **Figs. 9, 10, and 11,** respectively.

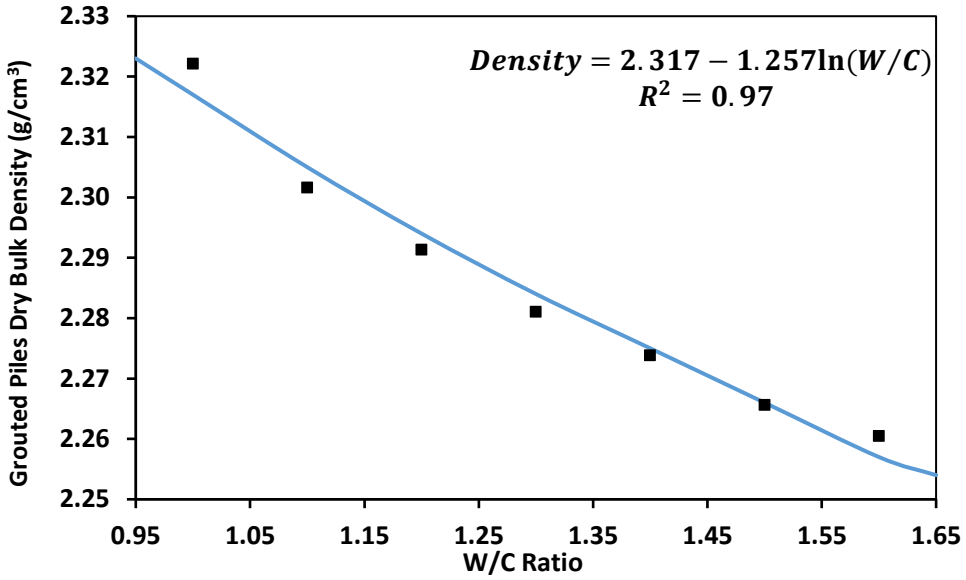


**Figure 9.** Grouted piles dry bulk density (g/cm$^3$) variation with the injected binder W/C ratio and the mathematical model relating the parameters

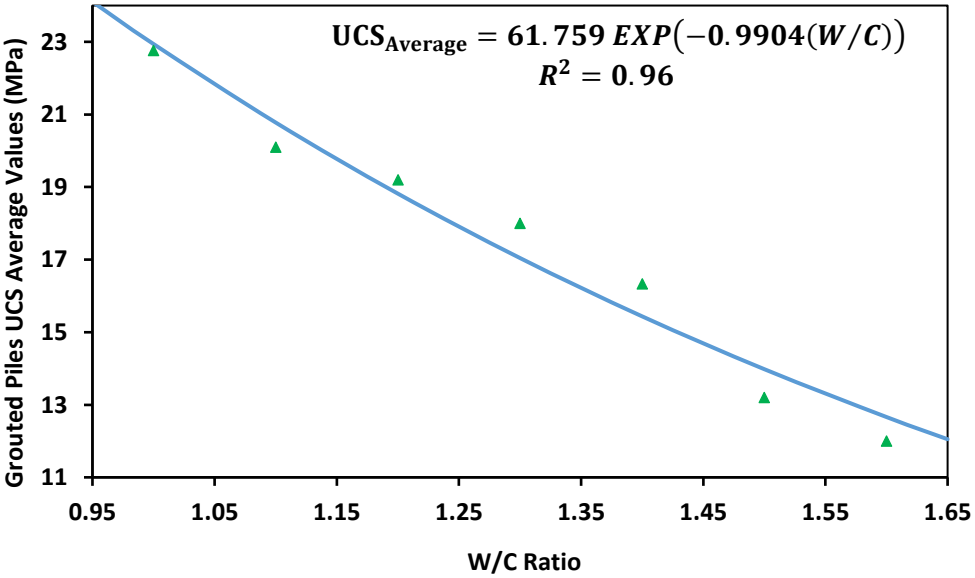


**Figure 10.** Grouted piles $UCS_{ave.}$ variation with the injected binder W/C ratio and the mathematical model relating the parameters

The previous relationships show that as the binder W/C ratio increases, the grouted pile samples' dry density, UCS, and E decrease. This is because the W/C ratio affects the hydration process of the cement grains, which is needed for the development of strength. After all, increasing the binder water/cement ratio leads to higher porosity for the excess water in the grouted pile microstructure and less quality in hardened grouted piles.

The high determination coefficients ($R^2$) of the above relations validate and assess the performance of the low-pressure injection laboratory device concerning the homogeneity

and reproducibility of the consistent grouted pile samples. The $R^2$ coefficient provides information about a mathematical model's goodness of fit. In the context of regression, it is a statistical measure of how well the regression line approximates the actual data. The values of $R^2$ for the mathematical models for the investigated relation were higher than 95 %, which shows a very close approximation to the real data.

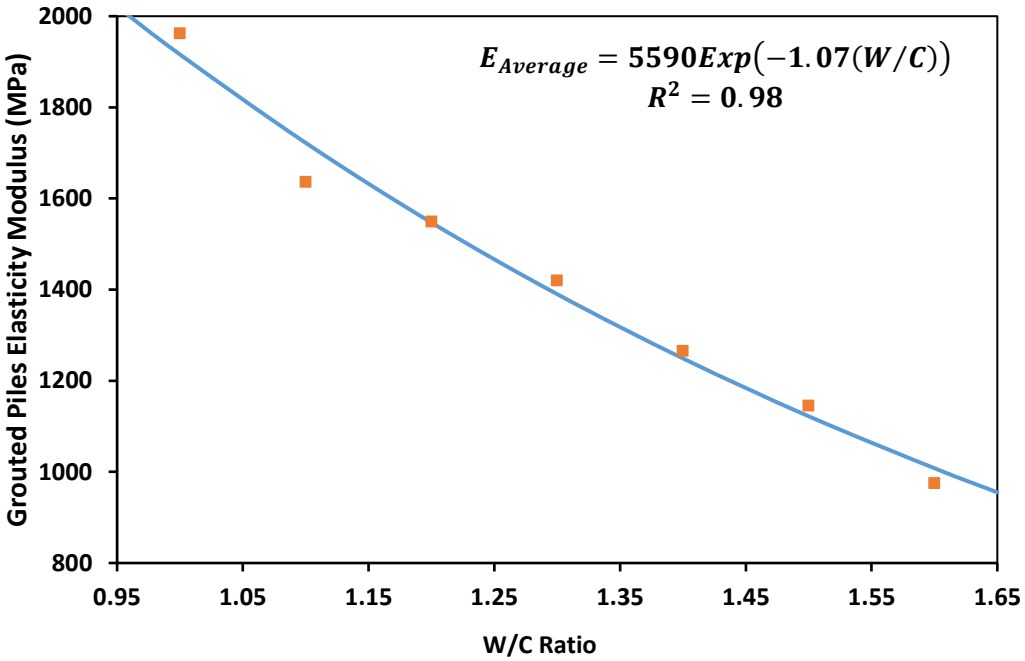


Figure 11. Grouted piles elastic modulus variation with binder W/C ratio and the mathematical model relating the parameters

**Fig. 12** shows the effect of the W/C ratios of the injected piles binders on the UCS-strain relations, where the lower W/C ratio of the injected binders, which means the minimum pores occupied by water in the grouted piles microstructure, leads to a higher UCS value and a stiffer stress-strain relation. Also, it can be seen from **Fig. 12** (Grouted piles UCS in MPa and Strain % relations for W/C ratios) that there is no conflict between these maximum values and the values of **Fig. 10** (Grouted piles in MPa and W/C ratio relation) simply because **Fig. 10** represents the average UCS values of the tested samples. In contrast, **Fig. 12** illustrates single sample data tests, which are within the range of the UCS average values.
As an apparent effect of adding SF to the injected binder mix of the grouted model piles, **Fig. 13** compares UCS results for both OPC only and SF + OPC binder mixtures. The tests showed that adding SF to the injected binder mixture results in about double the strength of the OPC-injected binder mixture because of the SF micro-filler and pozzolanic effects.

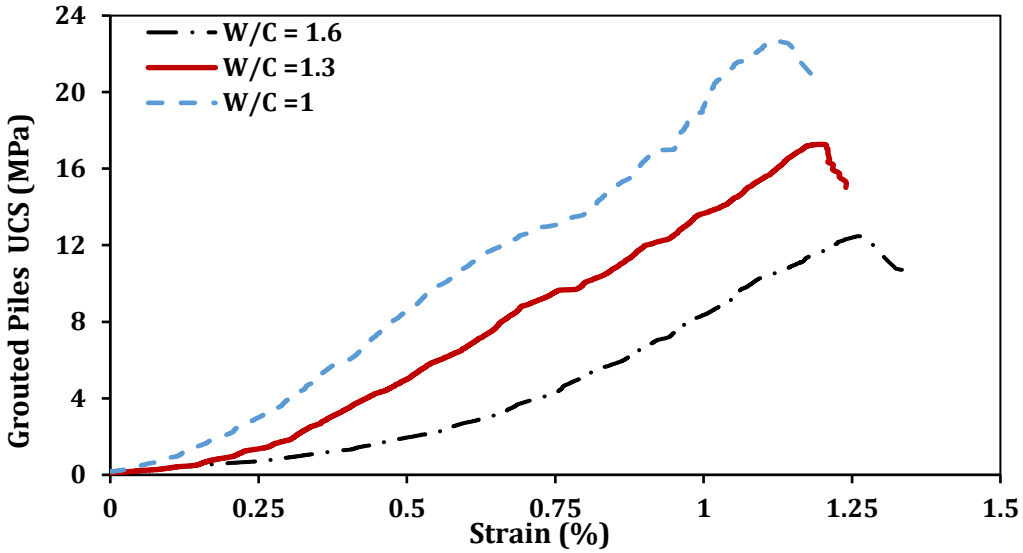


**Figure 12.** Grouted piles UCS-Strain relation for three different W/C ratios of the injected binder

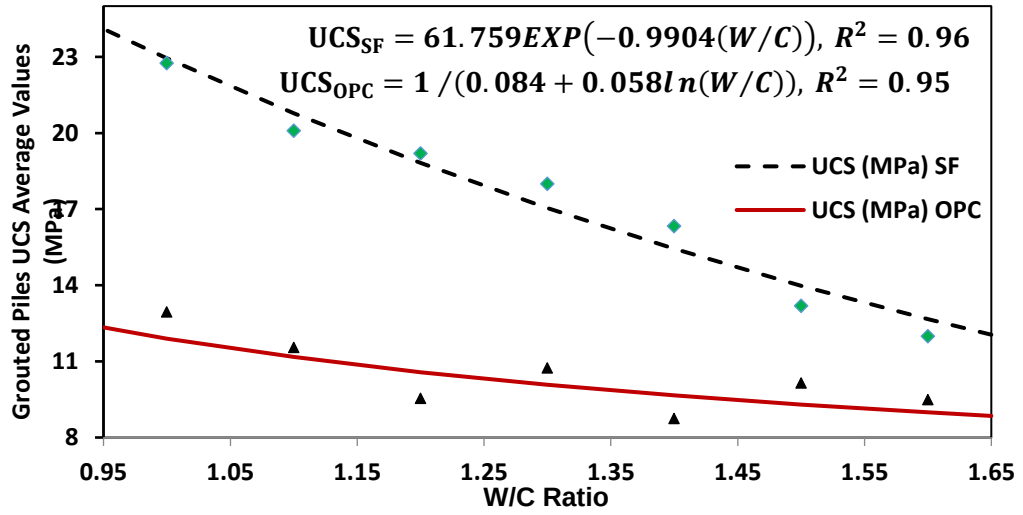


**Figure** 13. Comparison between the UCS-W/C ratio relations for grouted piles injected by (OPC and OPC cement + 10 % SF) with their mathematical models

## 4. CONCLUSIONS

In this study, the high determination coefficients ($R^2$) of the studied factors for randomly chosen samples of model piles grouted by the low-pressure injection laboratory device made it possible to assess its performance regarding the homogeneity and reproducibility of grouted samples. The next points summarize the study's main findings:

- Jet grout is complicated and partly defined, making grouted pile quality difficult to control. So, trial grouting occurs temporarily with similar project soil conditions. Grouting has been replicated in the lab using the same field tools on a reduced scale with identical soil conditions to replace costly, time-consuming, and ineffective field trial injections. So, a lab low-pressure injection setup was built to study the grout binder's soil injection ability on soil and the model piles' homogeneity.

- Based on the test results of the investigated factors (density, *E*, and UCS) of the pile models injected by the low-pressure laboratory setup, it was found that the W/C ratios and the addition of SF to the injected binder mixtures have an evident effect on the properties of the grouted pile based on a comparison of SF and OPC-injected binders with different W/C ratio mixtures.
- Adding SF to the injected binder mixture increases the UCS value of the grouted pile at the same W/C ratio (about double) compared to that mixture with only OPC because of the SF micro-filler and pozzolanic effects while increasing the W/C ratio for a specific binder mixture decreases the UCS, density, and E of the grouted pile because of the higher porosity in the microstructure formed by the excess water, leading to less quality in hardened grouted piles.
- For the binder injections with a W/C ratio of one and 10% SF additive by weight of cement mass, the highest grouted pile values were obtained for density, E, and UCS with about 2.32 g/cm$^3$, 23 MPa, and 2000 MPa, respectively.
- The consistent pile models were obtained after multiple low-pressure injection trials to establish the proper operating factors (binder injection pressure/flow rate, injection nozzle number and size, penetrating/lifting rate, and boring-grouting rod rotation speed).

## NOMENCLATURE

| Symbol | Description | Symbol | Description |
|---|---|---|---|
| $C_C$ | Curvature Coefficient | UCT | Unconfined Compressive Tests |
| $C_U$ | Uniformity Coefficient | W/C | water/cement ratio |
| $D_r$ | Soil relative density | UCS | Uniaxial Compression Stress |
| $E$ | Elasticity modulus | $\emptyset^\circ$ | Dry friction angle |
| $e_{max}$ | Maximum void ratio | $\gamma_d$ | The selected dry unit weight, |
| $e_{min}$ | Minimum void ratio | $\gamma_{dmax,}$ | The soil dry unit weight in densest conditions |
| SF | Silica Fume | $\gamma_{dmin}$ | The soil dry unit weight in the loosest conditions |

## REFERENCES

Akın, M., Akın, M., Çiftçi, A., and Bayram, B.B., 2015. The effect of jet grouting on the cyclic stress ratio (CSR) for the mitigation of liquefaction. *Ejoir*, 1, pp. 10-20.

Ali, H.A., and Yousuf, Y.M., 2016. Improvement of shear strength of sandy soil by cement grout with fly ash. *Journal of Engineering*, 22(12), pp. 16-34. Doi:10.31026/j.eng.2016.12.02.

AL-Malkee, F.W., and Ahmed, M.D., 2021. Laboratory study on the effect of water-cement ratio on strength characteristics of jet grouting columns. *Journal of Engineering*, 27(12), pp. 33-49. Doi:10.31026/j.eng.2021.12.04.

Al-Saidi, A.A., Al-Juari, K.A., and Fattah, M.Y., 2022. Reducing settlement of soft clay using different grouting materials. *Journal of the Mechanical Behavior of Materials*, 31(1), pp. 240-7. Doi:10.1515/jmbm-2022-0033.

ASTM-D2435/D2435M-11, 2011. Standard test method for one-dimensional consolidation properties of soils using incremental loading. Annual Book of ASTM (American Society of Testing Material) Standards, 4.

ASTM-D2166/D2166M-16, 2016. Standard Test Method for Unconfined Compressive Strength of Cohesive Soil. Philadelphia, PA, United States.

ASTM-D2487-11, 2011. Standard Practice for Classification of Soils for Engineering Purposes (Unified Soil Classification System). West Conshohocken, Pennsylvania (USAASTM).

ASTM-D3080/D3080M-11, 2011. Standard test method for direct shear test of soils under consolidated drained conditions.

ASTM-D422-63(2007), 2007. Standard test method for particle-size analysis of soils. American Society for Testing and Materials.

ASTM-D4253-14, 2014. Standard test methods for maximum index density and unit weight of soils using a vibratory table. American Society for Testing and Materials.

ASTM-D4254-16, 2016. Standard test methods for minimum index density and unit weight of soils and calculation of relative density. West Conshohocken PA.

ASTM-D4318-17, 2017. Standard test methods for liquid limit, plastic limit, and plasticity index of soils. ASTM International.

ASTM-D6913/D6913M-17, 2017. Standard Test Methods for Particle-Size Distribution (Gradation) of Soils Using Sieve Analysis. ASTM International, West Conshohocken, PA.

ASTM-D854-14,2014. Standard Test Methods for Specific Gravity of Soil Solids by Water Pycnometer. ASTM International. Pennsylvania, PA, USA.

Fattah, M.Y., Al-Ani, M.M., and Al-Lamy, M.T., 2013.Treatment of collapse of gypseous soils by grouting. Proceedings of the Institution of Civil Engineers-Ground Improvement. 166(1), pp. 32-43. Doi:10.1680/grim.11.00020.

Fattah, M.Y., Joni. H.H., and Abood, A.S., 2020. Erosion of dune sands stabilized by grouting with lime–silica fume mix. Proceedings of the Institution of Civil Engineers-Ground Improvement. 173(1), pp. 3-18. Doi:10.1680/jgrim.17.00026.

Fretti, C., Presti, D.L., and Pedroni, S., 1995. A pluvial deposition method to reconstitute well-graded sand specimens. *Geotechnical testing journal*, *18*(2), pp. 292-298. Doi:10.1520/GTJ10330J.

Guler, E., and Secilen, G.G., 2021. Jet grouting technique and strength properties of jet grout columns. In *Journal of Physics: Conference Series* (Vol. 1928, No. 1, P. 012006). IOP Publishing. Doi:10.1088/1742-6596/1928/1/012006.

Han, J., 2015. *Principles and practice of ground improvement*. John Wiley & Sons.

Hariprasad, C., Rajashekhar, M., and Umashankar, B., 2016. Preparation of uniform sand specimens using stationary pluviation and vibratory methods. *Geotechnical and Geological Engineering*, *34*, pp. 1909-1922. Doi:10.1007/s10706-016-0064-0.

Hasanzadeh, A., and Shooshpasha, I., 2019. Effects of silica fume on cemented sand using ultrasonic pulse velocity. *Journal of Adhesion Science and Technology*, *33*(11), pp. 1184-1200. Doi:10.1080/01694243.2019.1582890.

Holland, T.C., 2005. Silica fume–User's manual, US Department of Transportation. *Federal Highway Administration. Silica Fume Association (SFA),* 400 7th Street, SW. Washington, D20590.

Hossain, M.Z., and Ansary, M.A., 2018. Development of a portable traveling pluviator device and its performance to prepare uniform sand specimens. *Innovative Infrastructure Solutions*, *3*, pp. 1-12. Doi:10.1007/s41062-018-0159-y.

Hussein, S.H., and Ahmed, M.D., 2023. Stiffness characteristics of pile models for cement improving sandy soil by low-pressure injection laboratory setup. *Journal of Engineering*, *29*(3), pp. 154-169. Doi:10.31026/j.eng.2023.03.11.

Karkush, M.O., Ali, H.A., and Ahmed, B.A., 2018. Improvement of unconfined compressive strength of soft clay by grouting gel and silica fume. In Proceedings of China-Europe Conference on Geotechnical Engineering, 1, pp. 546-550. Doi:10.1007/978-3-319-97112-4_122.

Kumar, G.S., Sumanth, M.K., and Samuel, M., 2020. A review paper on stabilization of sandy soil using cement grouting technique. *Journal of Critical Reviews*, *7*(14), pp. 902-908. Doi:10.31838/jcr.07.14.160.

Lambe, T.W., and Whitman, R.V., 1991. *Soil mechanics* (Vol. 10). John Wiley & Sons. Doi:10.1177/030913338100500325.

Mohammed, M.S., Hussein, S.H., and Ahmed, M.D., 2023. Comparison between cement and chemically improved sandy soil by column models using low-pressure injection laboratory setup. *Journal of the Mechanical Behavior of Materials*, *32*(1), P.20220258. Doi:10.1515/jmbm-2022-0258.

Muller, A.C.A., Scrivener, K.L., Skibsted, J., Gajewicz, A.M., and McDonald, P.J., 2015. Influence of silica fume on the microstructure of cement pastes: New insights from 1H NMR relaxometry. *Cement and Concrete Research*, *74*, pp. 116-125. Doi:10.1016/j.cemconres.2015.04.005.

Njock, P.G., Shen, J.S., and Modoni, G., and Arulrajah, A., 2018. Recent advances in horizontal jet grouting (HJG): an overview. *Arabian Journal for Science and Engineering*, 43, pp. 1543-60. Doi:10.1007/s13369-017-2752-3.

Nikbakhtan, B., 2015. Development of thermal-insulating soilcrete using laboratory jet grouting setup [dissertation]. Edmonton, Canada: University of Alberta. Doi:10.7939/R3QR4NW4X.

Olgun, M., Kanat, A., Senkaya, A., and Erkan, I.H., 2021. Investigating the properties of jet grouting columns with fine-grained cement and silica fume. *Construction and Building Materials*, *267*, P.120637. Doi:10.1016/j.conbuildmat.2020.120637.

Reddy, C.V., and Ramadasu, T.L., 2017. Effect of silica fume on the compressive strength of cement-silica fume mortars. *International Journal of Current Engineering and Scientific Research (IJCESR)*, *4*(7), pp.13-21.

Schaefer, V.R., Mitchell, J.K., Berg, R.R., Filz, G.M., and Douglas, S.C., 2012. Ground improvement in the 21st century: a comprehensive web-based information system. In *Geotechnical Engineering State of the Art and Practice: Keynote Lectures from GeoCongress 2012* (pp. 272-293). Doi:10.1061/9780784412138.0011.

Wang, Z.F., Shen, S.L., Ho, C.E., and Kim, Y.H., 2013. Jet grouting practice: an overview. *Geotechnical Engineering Journal of the SEAGS & AGSSEA*, *44*(4), pp. 88-96.